47th AIAA Aerospace Sciences Meeting Including The New Horizons Forum and Aerospace Exposition
5 - 8 January 2009, Orlando, Florida

AIAA 2009-752

47th AIAA Aerospace Sciences Meeting Including The New Horizons Forum and Aerospace Exposition, 5-8 Jan 2009, Orlando, Florida

Forward-Blowing Plasma Actuation over Forebody Asymmetric Vortex

Zijie Zhao*, Huaxing Li†
Northwestern Polytechnical University, Xi'an 710072, China
Feng Liu‡, Shijun Luo§
University of California, Irvine, CA 92697-3975

Forward blowing from a pair of plasma actuators on the leeward surface and near the apex is used to switch the asymmetric vortex pair over a cone of semi-apex angle 10° at high angles of attack. The experiments were perfomed in a $3.0\ m \times 1.6\ m$ open-circuit wind tunnel at Reynolds number of 5×10^4 and 10^5 based on the cone base diameter. Pressure measurements show that by appropriate design of the actuators and appropriete choice of the a.c. voltage and frequency, side forces and yawing moments of opposite signs can be obtained at high angles of attack by activating one of the plasma actuators. Further study is suggested.

Nomenclature

C_m	=	pitching-moment coefficient about cone base, pitching moment/$q_\infty SD$
C_N	=	overall normal-force coefficient, overall normal-force/$q_\infty S$
C_{Nd}	=	local normal-force coefficient, local normal-force/$q_\infty d$
C_n	=	yawing-moment coefficient about cone base, yawing moment/$q_\infty SD$
C_p	=	pressure coefficient
C_Y	=	overall side-force coefficient, overall side-force/$q_\infty S$
C_{Yd}	=	local side-force coefficient, local side-force/$q_\infty d$
D	=	base diameter of circular cone forebody
d	=	local diameter of circular cone forebody
F	=	frequency of a.c. voltage source
L	=	length of circular cone forebody
q_∞	=	free-stream dynamic pressure
Re	=	free-stream Reynolds number based on D
S	=	base area of circular cone forebody
U_∞	=	free-stream velocity
U_{max}	=	maximum velocity induced by plasma actuator in still air
V_{p-p}	=	peak-to-peak voltage of a.c. voltage source
w	=	input power
α	=	angle of attack
θ	=	meridian angle measured from windward generator, positive when clockwise

*Graduate Student, Department of Fluid Mechanics.
†Professor, College of Aeronautical Engineering.
‡Professor, Department of Mechanical and Aerospace Engineering. Associate Fellow AIAA.
§Researcher, Department of Mechanical and Aerospace Engineering.

I. Introduction

The most interesting phenomena associated with high angle of attack aerodynamics is the sudden onset of vortex asymmetry on the forebody of an air vehicle in symmetric flight. One of the first observations of vortex asymmetry onset was reported in 1951 by Allen and Perkins.[1] Interest in the phenomenon has been intensified since the late 1970's as concepts for highly maneuverable aircraft have been developed. These high-performance aircrafts are expected to operate routinely at high angles of attack at which vortex asymmetry is known to occur. When vortex asymmetry occurs, the aerodynamic, stability, and control characteristics of the vehicle change dramatically. In the mean time, the conventional aerodynamic controls become ineffective due to the vortex wakes generated by the forebody.

High-angle-of-attack flow control is most effective when applied at the region close with the point apex of the forebody. The presence of two closely-spaced vortices around the pointed forebody at high angles of attack enhances the effectiveness. Compared with the wing, control on the forebody is required over a much small area and thus physical requirements such as size and weight could be much smaller. The lengthy forebody of a modern fighter further enhances the control effectiveness by providing a long moment arm. Excellent reviews of this activity can be found in papers by Malcolm[2,3] and Williams.[4]

Hanff, Lee and Kind[5] used the duty cycle modulation of the alternating blowing from two forward facing nozzles to control the mean lateral aerodynamic forces and moments over slender bodies. The method takes the advantage of the inherently bi-stable nature of the forebody vortices by deliberately switching them between their two stable states.

Flow control with electromagnetic energy addition receives significant attention, since it is fully electronic with no mechanical parts and has a broard frequency bandwidth so that it can have fast response for feedback control. It is highly desirable to replace the blowing nozzles in the method of Hanff et al.[5] with a pair of plasma actuators of single dielectric barrier discharge (SDBD).[6] The present paper is aimed at the study of a plasma flow control over a pointed slender forebody of revolution.

Asymmetric vortices on slender body of revolution have been reported.[7] Hall[8] established an inherent relation between the vortex flow and the surface pressure distribution on a slender body by comparing oil flow visualization and surface pressure measurements in the literature. In the following sections, the experimental setup is described. The experinental results are then presented and discussed. Finally conclusions are drawn.

II. Experimental Setup

The tests are conducted in an open-circuit low-speed wind tunnel at the Northwestern Polytechnical University. The test section has a 3.0 $m \times 1.6$ m cross section. The model is rigidly mounted onto the support in the test section shown in Fig. 1. A thorough job of cleaning the model was done prior to each run of the wind tunnel.

Since the nose of any pointed forebody is locally conical in shape, the flow may be regarded as locally equivalent to that about a tangent cone. The basic features of the asymmetric flow can be displayed by studying the flows over a circular cone. The experimental model is a circular cone of 10° semi-apex angle faired to a cylindrical afterbody. The length of the cone is 463.8 mm and the cone base diameter is 163.6 mm. The cone tip of length 150 mm is made of plastic for plasma-actuator accommondation and the rest of the model is made of metal.

The SDBD plasma actuators are designed small and compact so that they can be placed as close with the cone apex as possible and without mutual interference. Three different designs of the actutors and mounting schemes have been tested.[9,10] The one studied in this paper is shown in Fig. 2(a). The plasma actuator consists of two asymmetric copper electrodes of 0.03 mm thickness and a thin Kapton dielectric film wraps around the cone surface and separates the encapsulated electrode from the exposed electrode as shown in Fig. 2(b). The length of the electrodes is 7.3 mm. The width of the exposed and encapsulated electrode is 1 mm and 3 mm, respectively. The two electrodes are separated by a gap of 1.5 mm, where the plasma is created and emits a blue glow in darkness shown in Fig. 1(b). The effect of the SDBD actuator is to impart momentum to the flow like the forward facing nozzle used by Hanff et al.[5] but without the mass injection. The gap between the electrodes for our particular actuators was optimized for maximum induced air flow based on experiments conducted in still air outside the wind tunnel.

A pair of the SDBD actuators are mounted on the cone surface symmetrically. The side edges of the

(a) plasma off (b) port plasma on

Figure 1. The model in the wind tunnel.

(a) arrangement (b) SDBD

Figure 2. Sketches of the plasma actuators.

port-side electrodes are located at the meridian angle $\theta = 30^\circ$ and 120°, where θ is measured from the windward meridian of the cone and positive is clockwise when looking upstream. The leading edge of the exposed electrode is located at 25 mm from the cone apex. The plasma blows forward along meridians of the cone tip shown in Fig. 2. The encapsulated electrode is located below the exposed electrode so that the effect of the plasma is to induce a flow tangential to the cone surface toward the cone apex. (see arrows in Fig. 2.) The plasma-actuator arrangement is intended to push the tip vortex on the same side of the cone away from the cone surface. In the present study, the plasma actuators are made by hands and then attached to the cone tip surface with glue. The dielectric film wraps around the entire circumference. No allowance is made on the cone surface for the attachment.

Two modes of operations of the actuators are defined. The plasma-off mode corresponds to the case when neither of the two actuators is activated. The plasma-on mode refers to the conditions when either the port or starboard actuator is activated while the other is kept off during the test. These are called the port-on and starboard-on modes, respectively. Each of the two actuators on the cone model is separately driven by an a.c. voltage source (model CTP-2000K by Nanjing Suman Co.). The waveform of the a.c. source is sine wave. The peak-to-peak voltage and frequency are set at $V_{p-p} \approx 14\ kV$ and $F \approx 8.9\ kHz$, respectively. The measured power consumption is approximately 15 W.

Figure 3 compares the smoke lines for the plasma off and the port plasma on in still air outside the wind tunnel. The still-air experiments were conducted in a Plexiglas cover to shield the inside air from air flow within the laboratory. The air flow induced by the port plasma on is clearly shown in Fig. 3(b). The maximum speed of the induced flow on the plane perpendicular to the cone axis at the apex, U_{max}, was measured with a hot-wire anemometer survey. Fig. 4(a) shows the maximum speed, U_{max} vs. V_{p-p} at $F \approx 8.9\ kHz$. $V_{p-p} = 14\ kV$ is chosen for the present tests. Fig. 4(b) shows the sketch of the unwrapped plasma actuators before glued around the model tip surface.

(a) plasma off

(b) port plasma on

Figure 3. Comparison of the smoke lines for plasma off and port plasma on in still air.

Surface pressure measurements are chosen for the model instrumentation to maximum the information provided about the complex flow and to allow much rigid mounting of the model required for the high-angle-of-attack tests. The 252 pressure tappings are arranged in rings of 36, every 10° around the circumference of the cone, at 7 stations uniformly distributed from $x/L = 0.340$ to 0.813 on the cone forebody. Details can be found in Ref. 11. Pressure reading from the transducers 9816 and 8400 made by the PSI Company are taken 64 and 127 times per second, respectively. The computer system was set up to output one- and five-second averages. A comparison of the measurements reveal that there are no differences in the one-second and five-second average pressures in our experiments. We present the five-second average data below. Among the total 252 pressure taps, fewer than 10 were found to give abnormal pressure readings, which are removed and replaced by linearly interpolated values from neighboring normal readings in the data processing phase.

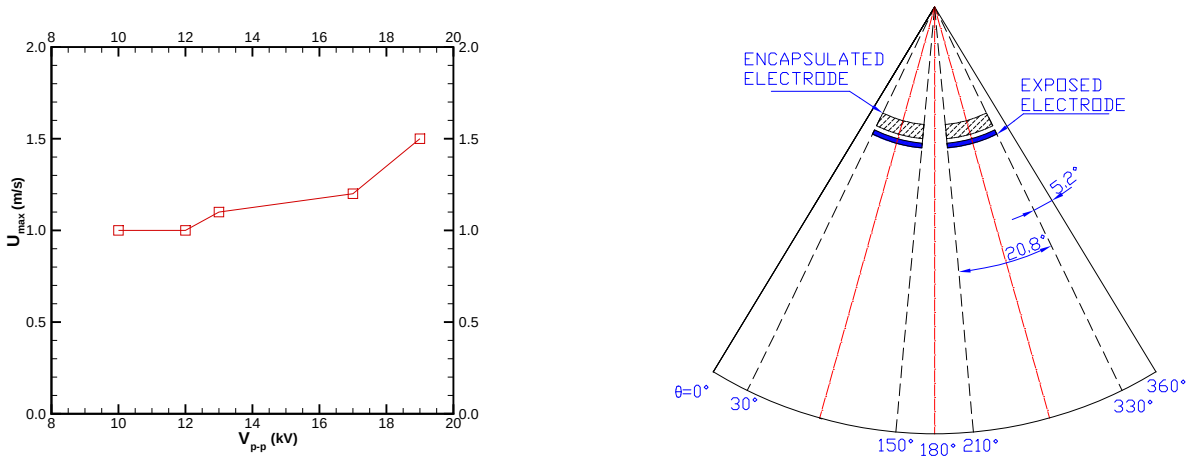

(a) maximum speed

(b) unwrapped plasma actuators

Figure 4. (a) Maximum speed of the plasma induced flow in still air. (b) Sketch of the unwrapped plasma actuators over the model tip surface.

III. Experimental Results and Discussions

In a typical bi-stable mode, the asymmetry may be either towards the starboard side or the port side, affected by slight imperfections of the cone near the apex and also free-stream conditions.[7] By taking advantage of the sensitivity of the flow on the conditions near the apex of the cone, we can control the vortex configuration and thus the pressure distribution asymmetry by activating one of the installed plasma actuators. Experiments were performed for the plasma-off, port-on and starboard-on. Three cases are presented: (1) $\alpha = 40°$ and $U_\infty = 5\ m/s$, (2) $\alpha = 45°$ and $U_\infty = 10\ m/s$, (3) $\alpha = 50°$ and $U_\infty = 5\ m/s$

A. Base Plasma-Off Flow at Zero Angle of Attack

In order to check the symmetry of the cone and model alignment in the wind tunnel, a test is run at zero angle of attack and with plasma off. Fig. 5 presents the pressure distributions at plasma off, $U_\infty = 5\ m/s$ and $10\ m/s$, and $\alpha = 0°$. Aside from some slight irregularities, the measured pressure distributions indicate essentially an axisymmetric flow around the cone. In the present study, the hand-made plasma actuators and no allowance for the attachment could have been the cause for the mentioned irregularities of the pressure distributions. Nevertheless, the disturbances were tolerably small.

B. Comparison of Plasma-Off and Plasma-On Results, $\alpha = 40°$

Figure 6 compares the pressure distributions for the plasma off and on at $\alpha = 40°$, $U_\infty = 5\ m/s$, Stations 1 and 7. The plasma-off pressure ditributions in Fig. 6 show that the suction peak on the port side of the cone is stronger than that on the starboard side of the cone, indicating that the port-side vortex is located closer with the cone than the starboard-side vortex.[8] The starboard-on distributions in Fig. 6 almost overlap with those of plasma-off. This is because the asymmetric perturbations produced by the starboard-side plasma actuator merely reassure the pre-existing plasma-off asymmetry of the flow. Activating the port-side plasma actuator, however, produces a desired switch of the asymmetry. The asymmetric surface pressure distributions shown in Fig. 6 switch sides. The port-on pressure distributions show stronger suction on the starboard side of the cone, indicating that the starboard-side vortex has moved close to the cone while the port-side vortex moved away from the cone. The port plasma actuator induces a momentum input in forward direction, which presumably pushes the port-side vortex away from the cone surface and, in the mean time, brings the starboard vortex with its feeding shear-layer close by the cone. Similar effects were observed by Hanff, et al.[5] Flow visualizations to reveal the detailed mechanism are suggested.

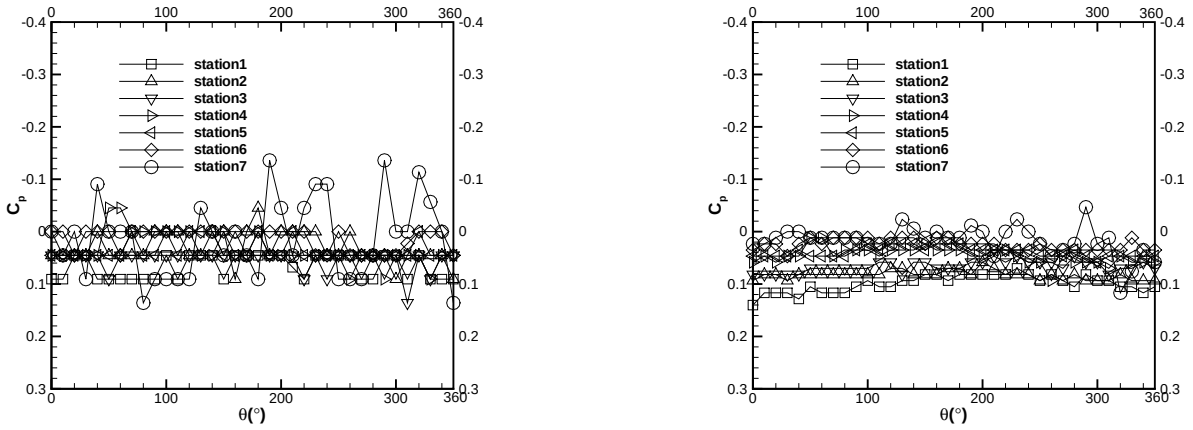

(a) $U_\infty = 5\ m/s$ (b) $U_\infty = 10\ m/s$

Figure 5. Comparison of pressure distributions at plasma off, $U_\infty = 5\ m/s$ and $10\ m/s$, and $\alpha = 0°$.

(a) station 1 (b) station 7

Figure 6. Comparison of pressure distributions for the plasma off and on at $\alpha = 40°$, $U_\infty = 5\ m/s$.

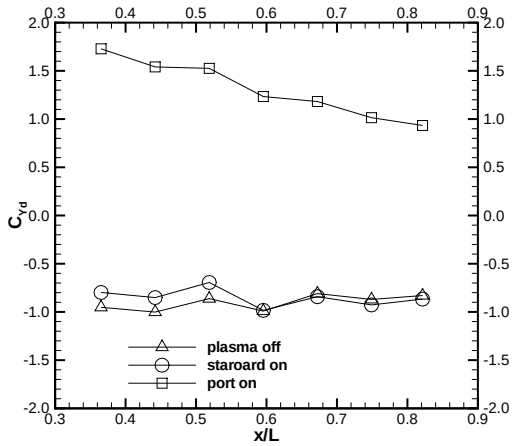

(a) local side force

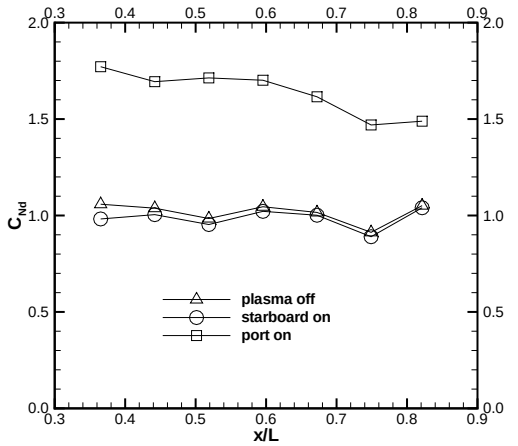

(b) local normal force

Figure 7. Comparison of local side- and normal-force distributions for the plasma off and on at $\alpha = 40°$, $U_\infty = 5\ m/s$.

The forces and moments acting on the cone forebody are calculated from the measured pressures by assuming that the pressure distributions are conical over each segment along the cone length which is divided by the mid points of the neighboring stations. The local forces are normalized with the local diameter of the cone. Figure 7 presents the distributions of the local side- and normal-force coefficients along the cone axis at $\alpha = 40°$, $U_\infty = 5\ m/s$. The local side- and normal-forces shown in Fig. 7 are nearly constant for each mode, indicating the cross-flow pattern remains similar along the cone axis. The starboard-on local side forces almost overlap with those of plasma-off, and they are negative. The port-on local side forces switch to positive, confirming that the stronger suction switches to the starboard side seen in Fig. 6. The local normal forces remain positive and have the same order of magnitudes of the local side forces.

The overall forces and moments are then calculated from the measured pressures and normalized with the area and diameter of the cone base. The moments are taken about the cone base. The yawing momoent is positive when yawing to the starboard side of the cone. Table 1 presents the overall force- and moment-coefficients for the three modes.

Table 1. Comparison of overall forces and moments for the plasma off and on at $\alpha = 40°$, $U_\infty = 5\ m/s$.

Item	C_Y	C_n	C_N	C_m
plasma-off	-1.1	-2.5	1.2	2.9
port-on	1.6	3.7	2.0	4.6
starboard-on	-1.0	-2.4	1.2	2.8

C. Comparison of Plasma-Off and Plasma-On Results, $\alpha = 45°$

Figure 8 compares the pressure distributions for the plasma off and on at $\alpha = 45°$, $U_\infty = 10\ m/s$, Stations 1 and 7. The plasma-off pressure distributions in Fig. 8 are almost symmetric, indicating that the vortex pair over the cone is almost symmetric. For the model Fig. 6 shows that the plasma-off pressure distributions are asymmetric. This deviation is understandable as the change in angle of attack and free-stream velocity may alter the small perturbations in the flow and, thus, result in different vortex pattern. In the present case the starboard plasma pressure distributions show stronger suction on the port side of the cone, while the port plasma pressure distributions has stronger suction on the starboard side of the cone. Both starboard- and port-on modes are effective in the present case, indicating that the momentum input induced by one-side actuator is capable to push the same-side tip vortex to move away from the cone surface and, in the same time, brings the other-side vortex with its feeding shear-layer close by the cone.

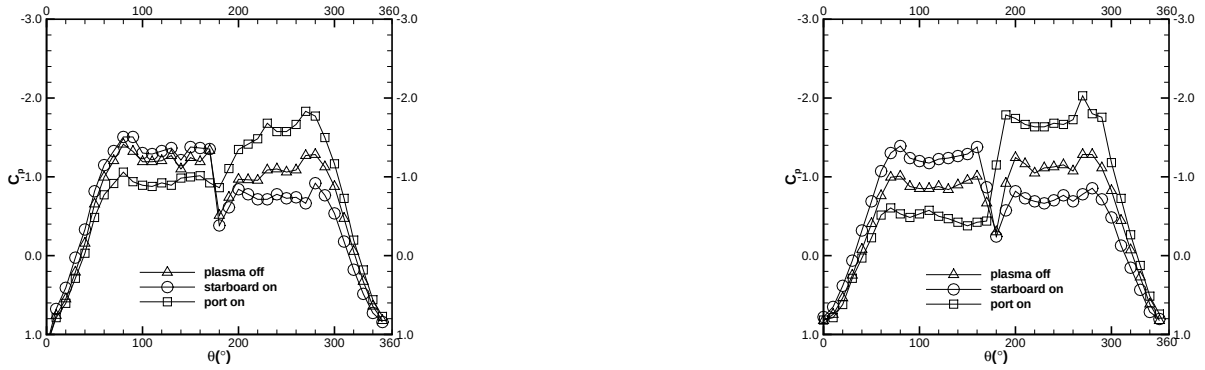

(a) station 1

(b) station 7

Figure 8. Comparison of pressure distributions for the plasma off and on at $\alpha = 45°$, $U_\infty = 10\ m/s$.

Figure 9 presents the local side- and normal-force acting on the cone forebody versus x/L at $\alpha = 45°$, $U_\infty = 10\ m/s$. The plasma-off local side forces nearly vanish. The local side forces for starboard on are negative, and those for port on are positive, similar to the previous case. The local normal forces are almost equal for plasma on and off, and of the same order of magnitudes of the two extreme local side forces. Table 2 presents the corresponding overall forces and moments.

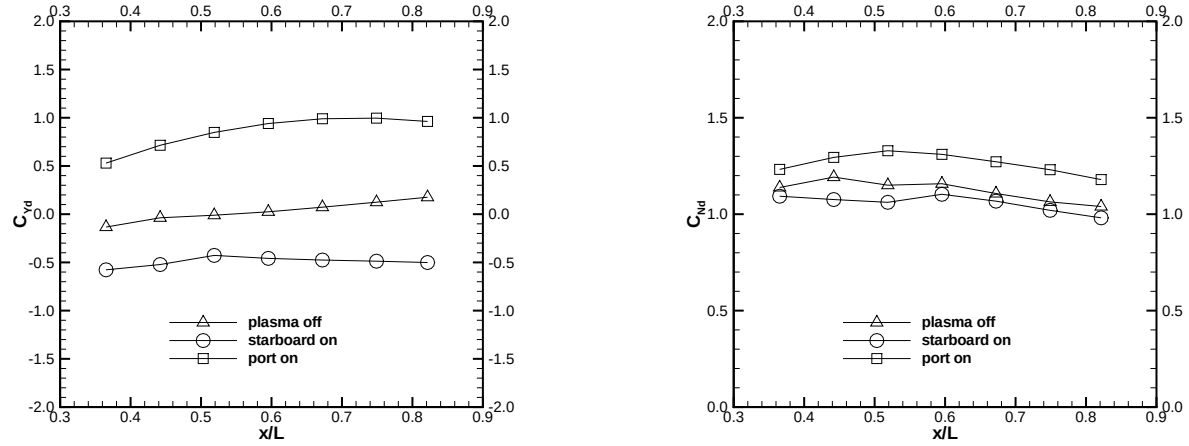

(a) local side force

(b) local normal force

Figure 9. Comparison of local side- and normal-force distributions for the plasma off and on, $V_{p-p} \approx 12\ kV$, $F \approx 8.9\ kHz$, $w \approx 15\ W$ at $\alpha = 45°$, $U_\infty = 10\ m/s$.

Table 2. Comparison of overall forces and moments for the plasma off and on at $\alpha = 45°$, $U_\infty = 10\ m/s$.

Item	C_Y	C_n	C_N	C_m
plasma-off	0.04	0.1	1.4	3.1
port-on	1.0	2.4	1.5	3.5
starboard-on	−0.61	−1.4	1.3	3.0

D. Comparison of Plasma-Off and Plasma-On Results, $\alpha = 50°$

Figure 10 compares the pressure distributions for the plasma off and on at $\alpha = 50°$, $U_\infty = 5\ m/s$, Stations 1 and 7. The plasma-off pressure distributions in Fig. 10 become asymmetric again, but the stronger suction appears on the starboard side of the cone in this case. In Fig. 10 the port-on distributions almost overlap with those of plasma-off. This is because the port-side plasma actuation merely reassures the pre-existing plasma-off vortex pattern in which the port-side vortex is located far away from the cone surface. The starboard-on pressure distributions show stronger suction on the port side of the cone, indicating that the starboard-side plasma actuation pushes the starboard vortex to move away from the cone and, thus, the port-side vortex moves close with the cone surface.

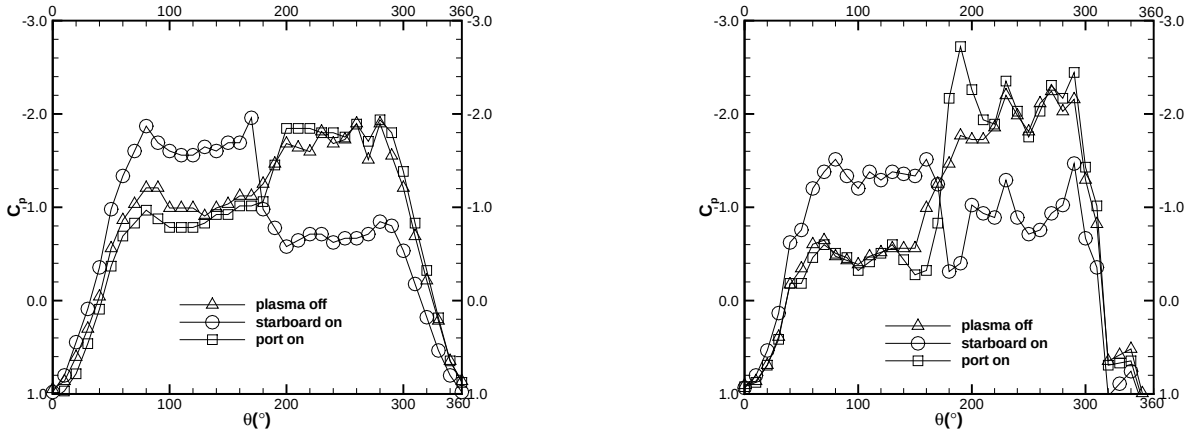

(a) Station 1

(b) Station 7

Figure 10. Comparison of pressure distributions for the plasma off and on at $\alpha = 50°$, $U_\infty = 5\ m/s$.

Figure 11 presents the local side- and normal-force acting on the cone forebody versus x/L at $\alpha = 50°$, $U_\infty = 5\ m/s$. Table 3 gives the corresponding overall force and moments. They confirm the pressure-distribution features shown in Fig. 10.

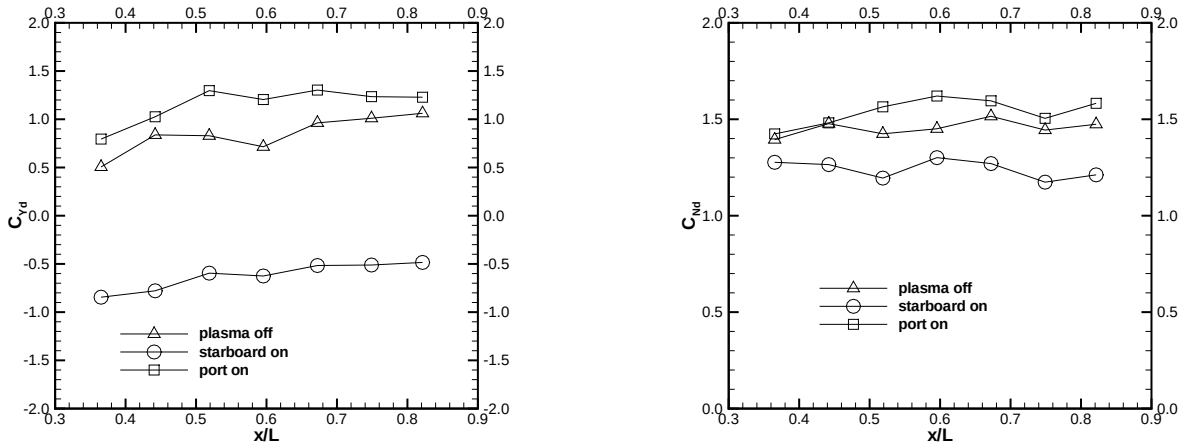

(a) local side force

(b) local normal force

Figure 11. Comparison of local side- and normal-force distributions for the plasma off and on at $\alpha = 50°$, $U_\infty = 5\ m/s$.

Table 3. Comparison of overall forces and moments for the plasma off and on at $\alpha = 50°$, $U_\infty = 5\ m/s$.

Item	C_Y	C_n	C_N	C_m
plasma-off	1.0	2.4	1.8	4.1
port-on	1.4	3.2	1.9	4.3
starboard-on	−0.76	−1.8	1.5	3.5

E. Summary of Lateral Force and moment, $\alpha = 40° - 50°$

Figure 12 summarizes the overall side force and yawing moment over $\alpha = 40° - 50°$ for plasma off and on. Although the free-stream velocity for $\alpha = 45°$ is $10\ m/s$ which is high than that for the other two angles of attack of $5\ m/s$, the comparison of their results still could be meaningful. As angle of attack is increased, the lateral forces for plasma-off change sign, while the lateral forces for starboard on and port on remain negative and positive througout the entire range of angle of attack, respectively. Therefore, it is feasible to achieve any intermediate lateral forces and moments between the two opposite extreme values by employing the present forward-blowing plasma actuators modulated with a duty-cycle technique.[9]

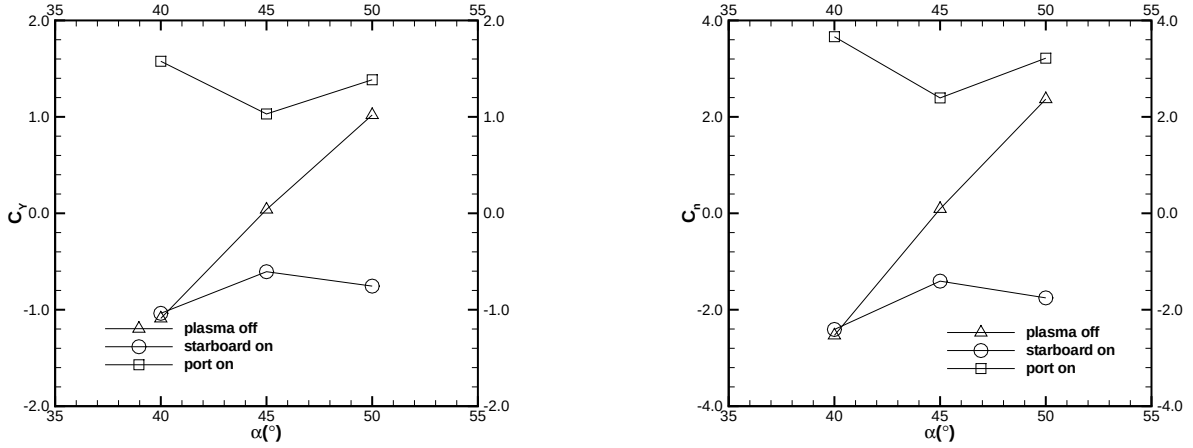

(a) overall side force

(b) yawing moment

Figure 12. Overall side force and yawing moment vs. angle of attack for plasma off and on conditions.

The starboard-on and the port-on forces and moments shown in Fig. 12 are opposite in sign but not exactly equal in amplitude at a given angle of attack. Among other factors, the imperfections of the model, particularly those due to the installment of the plasma actuators mentioned earlier, are believed to have prevented the results from following the presumed exact bi-stable behavior. Nevertheless, our pressure and force data clearly demonstrate the effectiveness of the plasma actuators in controlling bi-stable vortex flow patterns.

IV. Conclusions

Opposite lateral forces and moments over a slender conical forebody at high angles of attack has been demonstrated by employing a pair of forward-blowing single-dielectric-barrier-discharge plasma actuators near the cone apex. The plasma actuators impart momentum in forwrad direction to the flow. When properly located on the cone surface, they manipulate the relative position of the separation vortices over the forebody. It is feasible to achieve any intermediate lateral forces and moments between the two opposite extreme values at high angles of attack by employing the present plasma actuators modulated with a duty-cycle technique. Further investigations should be pursued to study more angles of attack, the detailed flow mechanism and to refine and optimize the design of the actuators.

Acknowledgment

The present work is supported by the Foundation for Fundamental Research of the Northwestern Polytechnical University, NPU-FFR-W018101.

References

[1]Allen, H. J. and Perkins, E. W., "A study of the effects of viscosity on the flow over slender inclined bodies of revolution," NACA TR 1048, 1951.

[2]Malcolm, G., "Forebody vortex control," *Prog. Aerospace Sci.*, Vol. 28, 1991, pp. 171–234.

[3]Malcolm, G., "Forebody vortex control–a progress review," AIAA Paper 93-3540, Aug. 1993.

[4]Williams, D., "A review of forebody vortex control scenarios," AIAA Paper 97-1967, June 1997.

[5]Hanff, E., Lee, R., and Kind,R.J., "Investigations on a dynamic forebody flow control system," Proceedings of the IEEE Conference, 1999, 99-0-7803-5715-9, pp. 28.1–28.9.

[6]Post, M., "Plasma actuators for separation control on stationary and oscillating airfoils," Ph.D Dissertation, University of Notre Dame, 2004.

[7]Zilliac, G. G., Degani, D., and Tobak, M., "Asymmetric vortices on a slender body of revolution," *AIAA Journal*, Vol. 29, No. 5, May 1991, pp. 667–675.

[8]Hall, R.M., "Influence of Reynolds number on forebody side forces for 3.5-diameter tangent-ogive bodies," AIAA-87-2274, Jun. 1987

[9]Liu, F., Luo, S.J.,Gao, C., Meng, X.S., Hao, J.N., Wang, J.L. and Zhao, Z.J., "Duty Cycle Plasma Flow Control over a Circular Cone Forebody," AIAA-2009-1082, Jan. 2009.

[10]Wang, J.L., Li, H.X., Liu, F. and Luo, S.J., "Forebody Asymmetric Load Manipulated by a Horseshoe-Shaped Plasma Actuator," AIAA-2009-0904, Jan. 2009.

[11]Meng, S. , Qiao, Z., Gao, C., Luo, S., and Liu, F, "Reynolds number effects on cone forebody side force," AIAA Paper 2008-4303, June 2008.